Flattening-induced electronic changes in zigzag single- and multi-walled boron nitride nanotubes: A first-principles DFT study

Y. Kinoshita,[1,2,*] S. Hase,[1] and N. Ohno[1,2]

[1]*Department of Computational Science and Engineering, Nagoya University, Furo-cho, Chikusa-ku, Nagoya 464-8603, Japan*

[2]*Department of Mechanical Science and Engineering, Nagoya University, Furo-cho, Chikusa-ku, Nagoya 464-8603, Japan*

(Received 1 May 2009; revised manuscript received 18 August 2009; published 17 September 2009)

Electronic structures of flattened (5,0), (13,0), and (21,0) single-walled (SW), (5,0)@(13,0) and (13,0)@(21,0) double-walled (DW), and (5,0)@(13,0)@(21,0) triple-walled (TW) boron nitride nanotubes (BNNTs) are investigated by performing first-principles calculations. The energy band and charge distribution of the BNNTs are calculated within the density-functional theory. Our calculations show that in the SWBNNTs, the energy of the conduction-band minimum (CBM) decreases with increasing flattening deformation, while that of the valence-band maximum hardly changes, resulting in monotonic decrease in the energy gap. The decrease in the energy of the CBM is caused by formation of bonds between neighboring boron atoms in curved regions. This tendency is found to be also true for the (13,0)@(21,0) DWBNNT but it exhibits more rapid decrease in the energy gap than in the SWBNNTs. In contrast, our results reveal that in the (5,0)@(13,0) DWBNNT and the (5,0)@(13,0)@(21,0) TWBNNT, the energy gap first increases and then decreases. It is found that this initial increase and subsequent decrease are caused by a charge spreading from the first to the second innermost tube and by formation of bonds in curved regions in the second innermost tube, respectively.

DOI: 10.1103/PhysRevB.80.125114 PACS number(s): 73.22.−f, 61.48.De, 71.15.Mb

I. INTRODUCTION

Boron nitride nanotubes (BNNTs) (Ref. 1) consist of alternately arranged boron and nitrogen atoms and have six-membered ring structure[2] similar to that of a carbon nanotube (CNT).[3] BNNTs were theoretically predicted in 1994 (Refs. 4 and 5) and were first experimentally synthesized in 1995.[1] Since then, as Golberg *et al.*[6] have reviewed, many synthetic techniques have been developed to produce BNNTs. Experimental and theoretical studies conducted thus far have shown that BNNTs prefer the double-walled (DW) or multi-walled (MW) structure with a zigzag atomic configuration to the single-walled (SW) one.[6] The zigzag type is denoted as $(n,0)$ and has a tube diameter of $\sqrt{3}an/\pi$, where a is the nearest interatomic distance between boron and nitrogen atoms. High-resolution transmission electron microscopy (HRTEM) images obtained by Golberg *et al.*[7–11] have demonstrated that the interwall spacing in MWBNNTs is in the range of 0.33–0.34 nm. First-principles calculations by Okada *et al.*[12] have verified that MWBNNTs with $n^{i+1}-n^i=8$ are energetically most stable, where i indicates the ith tube from the innermost one. BNNTs have high mechanical strength[13,14] and thermochemical stability.[15] The primary reason why BNNTs have attracted attention is that unlike CNTs, BNNTs are electrically insulating, independent of their diameters, chiralities, and the number of walls.[6] Thus, BNNTs are expected to be used as electrical insulation coatings for metallic or semiconducting nanochains, nanowires, and nanotubes. In particular, BNNTs should have high applicability under severe conditions, such as high temperatures and chemically hazardous environments.

However, Bai *et al.*[16] have recently found experimentally that the electrical transport property of a MWBNNT changes from insulating to semiconducting when a bending deformation is introduced and observed using HRTEM that the bending is accompanied by local flattening. Prior to this experiment, Kim *et al.*[17] have investigated energy gaps of flattened (9,0) zigzag and (5,5) armchair SWBNNTs by first-principles calculations. Their results have revealed that the energy gap of the (5,5) BNNT hardly changes but that of the (9,0) BNNT decreases with increasing flattening deformation. A first-principles study by Peng *et al.*[18] has shown that the energy gap of the (9,0) SWBNNT is insensitive to axial strain. Their results indicate that the usefulness of BNNTs as nanocoatings might be lost under certain conditions (e.g., warpage caused by thermal stress). An alternative view is that BNNTs can be used in nanoelectronic devices by introducing a deformation. In any case, further studies on electronic structures of deformed BNNTs are essential. At present, because deformation analyses of SWBNNTs, except for (9,0) and (5,5) BNNTs, and MWBNNTs have not been performed, the effects of tube diameters and interwall interactions on deformation-induced electronic changes in BNNTs remain unknown.

In this study, we examine electronic structures of flattened (5,0), (13,0), and (21,0) SW, (5,0)@(13,0) and (13,0)@(21,0) DW, and (5,0)@(13,0)@(21,0) triple-walled (TW) BNNTs by first-principles density-functional theory (DFT) calculations and discuss the mechanism of flattening-induced electronic changes in BNNTs. It is shown that the energy gap of the (5,0)@(13,0) DW and (5,0)@(13,0)@(21,0) TWBNNTs first increases and then decreases with increasing flattening deformation, while that of the SWBNNTs monotonically decreases, indicating that interwall interactions have a significant effect on the electronic structures of flattened BNNTs.

II. SIMULATION PROCEDURE

In the present study, we focus on (5,0), (13,0), and (21,0) SW, (5,0)@(13,0) and (13,0)@(21,0) DW, and (5,0)@(13,0)@(21,0) TWBNNTs. Figure 1 shows the simulation model of the (13,0)@(21,0) DWBNNT. The initial

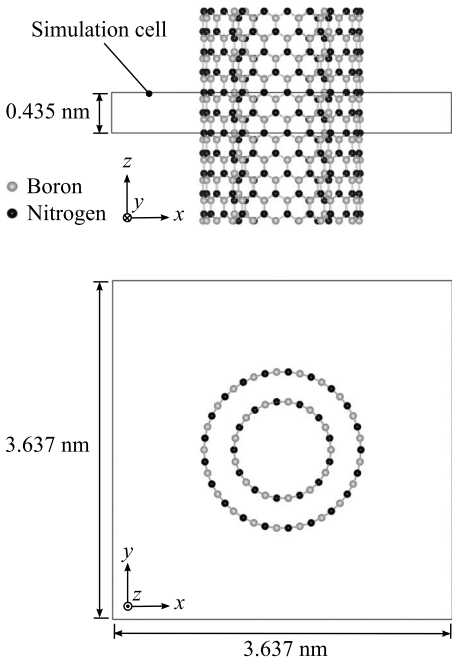

FIG. 1. Simulation model of (13,0)@(21,0) DWBNNT.

nearest interatomic distance between boron and nitrogen atoms is set as 0.145 nm. Boron (nitrogen) atoms in the outer tube are stacked above nitrogen (boron) atoms in the inner tube.[19] The axial direction of the BNNT is parallel to the z direction. The BNNT is located at the center of the unit cell with a size of 3.637 nm$\times$3.637 nm$\times$0.435 nm. Even though a three-dimensional periodic boundary condition is employed, the cell sizes in the x and y directions are large enough to avoid interaction with neighboring image cells, because they have little effect (less than 1%) on the energy, charge distribution, and energy-band structure of a flattened BNNT, when they are greater than the diameter of the BNNT plus 1.0 nm.

Atomic positions and the cell size in the z direction are first relaxed using the conjugate gradient method until atomic forces and the stress component, σ_{zz}, become less than 0.01 eV/Å and 0.01 GPa, respectively. After obtaining the equilibrium structure, a flattening compression in the x direction is applied by reducing the distance between imaginary walls until the BNNT collapses (Fig. 2). Once an atom contacts a wall, the atom is allowed to move only on the wall. During compression, the cell sizes are fixed and atomic configurations are relaxed until their forces become less than 0.01 eV/Å. To investigate the degree of deformation, the flattening ratio, η, is defined as

$$\eta = \frac{D_0 - D}{D_0}, \tag{1}$$

where D_0 is the diameter of the outermost tube at equilibrium and D is the distance between the imaginary walls.

We conduct first-principles DFT calculations using the Vienna *ab initio* Simulation Package (VASP).[20,21] The wave functions are expanded in a plane-wave basis set with a cutoff energy of 350 eV. The ultrasoft pseudopotential proposed

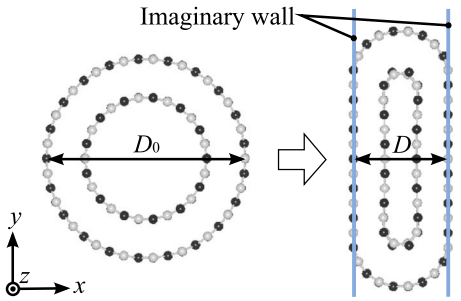

FIG. 2. (Color online) Schematic illustration explaining flattening compression of BNNTs.

by Vanderbilt[22] is used and the exchange-correlation energy is evaluated by the generalized gradient approximation of Perdew and Wang.[23] The Brillouin-zone integration is performed by the Monkhorst-Pack scheme[24] using a $1\times1\times4$ k-point mesh.

III. RESULTS AND DISCUSSION

From the energy variation with deformation, the lateral forces required to flatten the BNNTs to η=0.4 were estimated to be 6.8, 1.0, 0.6, 12.5, 2.5, and 14.7 nN for (5,0) SW, (13,0) SW, (21,0) SW, (5,0)@(13,0) DW, (13,0)@(21,0) DW, and (5,0)@(13,0)@(21,0) TWBNNTs, respectively, which are not unrealistic.[25]

Figure 3 shows the change in the energy-band structures of the (13,0) SWBNNT and (13,0)@(21,0) and (5,0)@(13,0) DWBNNTs during flattening deformation. The other SWBNNTs and the (5,0)@(13,0)@(21,0) TWBNNT show a similar changing trend of the band structure to the (13,0) SWBNNT and the (5,0)@(13,0) DWBNNT, respectively. Both the valence-band maximum (VBM) and the conduction-band minimum (CBM) of the (13,0) SWBNNT and (13,0)@(21,0) DWBNNT are located at the Γ point (k =0) during the deformation but those of the (5,0)@(13,0) DWBNNT move to $k\neq0$ midway during the deformation and then return to the Γ point. In each BNNT, the energy of the VBM, E_{VBM}, hardly changes, while that of the CBM, E_{CBM}, changes, indicating that the change in the energy gap, E_{g}, is mainly caused by a change in E_{CBM}. In the (13,0) SW and (13,0)@(21,0) DWBNNTs [Figs. 3(a) and 3(b)], E_{CBM} decreases monotonically. In contrast, in the (5,0)@(13,0) DWBNNT [Fig. 3(c)], E_{CBM} first increases and then decreases.

Figure 4 shows the energy gaps of the (5,0), (13,0), and (21,0) SWBNNTs, (5,0)@(13,0) and (13,0)@(21,0) DWBNNTs, and (5,0)@(13,0)@(21,0) TWBNNT as a function of the flattening ratio. The energy gap of the three SWBNNTs decreases almost monotonically and the amount of decrease becomes smaller with increasing tube diameter. The energy gap of the (13,0)@(21,0) DWBNNT also decreases monotonically but it exhibits a more rapid decrease than the (13,0) and (21,0) SWBNNTs. It should be noted that the energy gaps of the (5,0)@(13,0) DWBNNT and (5,0)@(13,0)@(21,0) TWBNNT increase during the early stage and then decrease. This shift occurs earlier in the latter

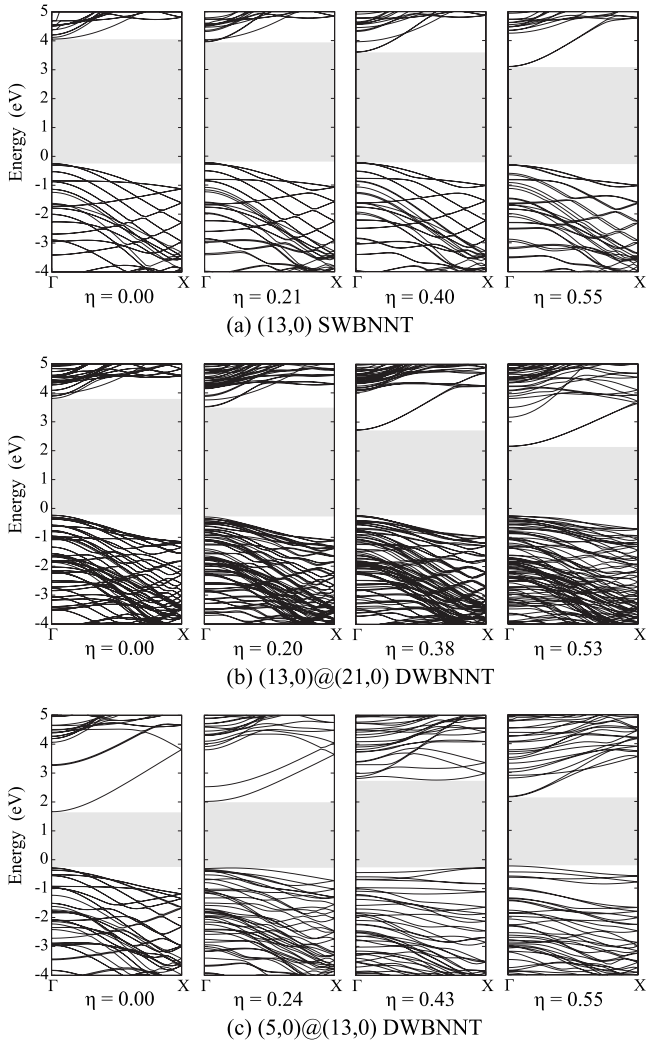

FIG. 3. Change in the band structure of (13,0) SWBNNT and (13,0)@(21,0) and (5,0)@(13,0) DWBNNTs in flattening deformation. The origin of the energy scale is set at the Fermi level.

(η=0.34) than in the former (η=0.48). The fact that the (5,0)@(13,0) DWBNNT and (5,0)@(13,0)@(21,0) TWBNNT show different changing trends of E_g from the SWBNNTs proves that interwall interactions significantly affect the electronic structures of the flattened (5,0)@(13,0) DWBNNT and (5,0)@(13,0)@(21,0) TWBNNT.

It is important to note that Fig. 4 represents only a qualitative trend because it is well known that calculations based on the DFT underestimate the energy gap. For a quantitative discussion of the energy gap, a modified theory such as the GW approximation (GWA) is necessary.[26–29] Nonetheless, previous studies on bulk hexagonal BN and an isolated BN sheet have shown that energy-band structures calculated by the DFT agree qualitatively well with those by the GWA.[26,27] For these reasons, the GWA is expected to shift the curves in Fig. 4 upward without dramatic changes in their shapes.

Figure 5 shows charge densities at the CBM of the flattened (5,0), (13,0), and (21,0) SWBNNTs at a cross section passing through boron atoms. The characteristics of the nearly free-electron (NFE) state are observed in the BNNTs with a small curvature [Fig. 5(b): η=0.00, (c): η=0.00, 0.20]

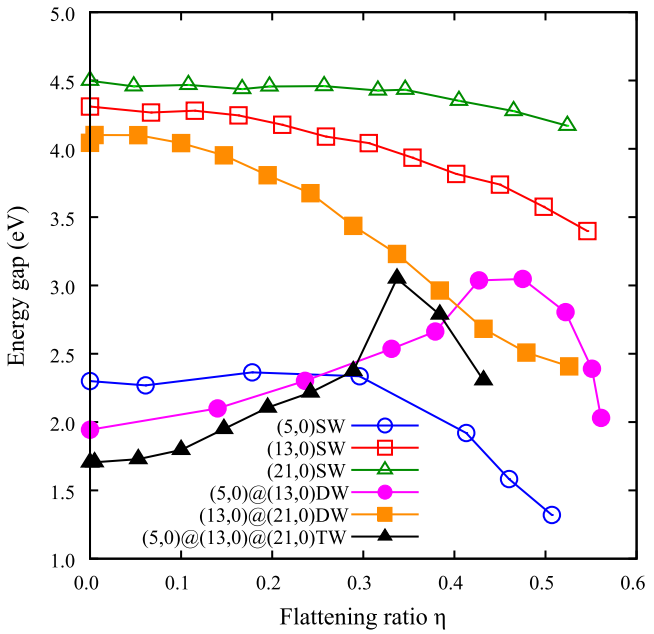

FIG. 4. (Color online) Relationship between energy gap, E_g, and flattening ratio, η, of (5,0), (13,0), and (21,0) SWBNNTs, (5,0)@(13,0) and (13,0)@(21,0) DWBNNTs, and (5,0)@(13,0)@(21,0) TWBNNT.

while π^*-σ^* hybridizations appear in the others. The reason the CBM of the (13,0) and (21,0) SWBNNTs changes from a NFE-like state to a π^*-σ^* hybridized state is that the tube curvature increases locally as the flattening deformation increases [in $(n,0)$ SWBNNTs under no deformation, the CBM is a NFE-like state when $n \geq 13$ and a π^*-σ^* hybridized state when $n < 13$, and the hybridization becomes stronger with increasing tube curvature].[5] The energy gap of the (5,0) SWBNNT is much smaller than those of the (13,0) and (21,0) SWBNNTs because of its strong π^*-σ^* hybridization. With increasing flattening deformation, charge is transferred from flattened regions to curved ones, leading to an overlap of the charge densities. The E_{CBM} of the SWBNNTs decreases under flattening because of the formation of electronic bonds between neighboring boron atoms in the curved regions. The charge-density distribution in curved regions of the (13,0) SWBNNT at η=0.21 is similar to that of the (21,0) SWBNNT at η=0.52, which results in them having almost the same energy gap of 4.2 eV. This is because they have almost the same value of D, namely, the same curvature of the curved region. Figure 6 shows the relationship between the energy gap and imaginary wall distance of the (13,0) and (21,0) SWBNNTs. Their energy gaps are almost equal under a same wall distance. Comparing the charge densities at a η of about 0.5 in Fig. 5, we see that the bonds weaken as the tube diameter increases. Therefore, a SWBNNT with a larger diameter shows a smaller amount of decrease in E_{CBM} under flattening or a lower rate of decrease in E_g.

The CBM charge-density distribution of the (13,0)@(21,0) DWBNNT is similar to that of the SWBNNTs (Fig. 7). In the inner tube, charge transfer from flattened to curved regions is observed and an overlap of the charge den-

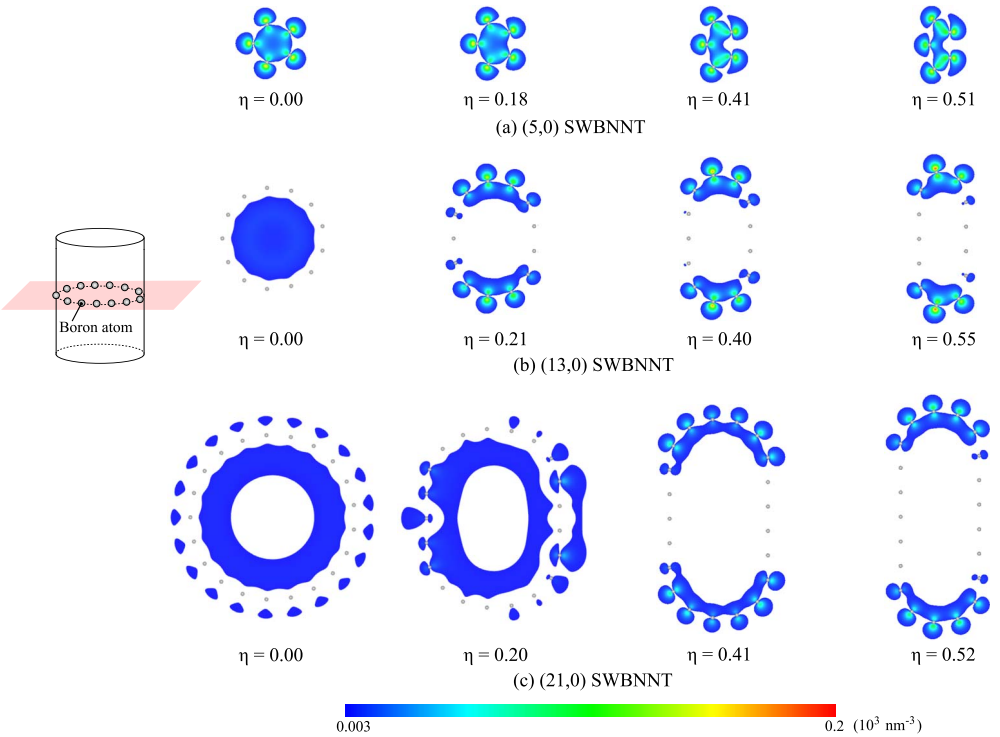

FIG. 5. (Color online) Change in the CBM charge density of (5,0), (13,0), and (21,0) SWBNNTs in flattening deformation.

sities is induced in the curved regions. The decrease in E_{CBM} of the (13,0)@(21,0) DWBNNT is caused by the same mechanism as in the SWBNNTs mentioned above. Because the charge densities are distributed almost entirely in the inner tube during deformation, one might expect that the $E_g - \eta$ curve of the (13,0)@(21,0) DWBNNT coincides with that of the (13,0) SWBNNT. However, E_g of the former is in fact smaller than that of the latter under the same η. As shown in Fig. 7, the flattening ratio of the innermost tube, η_{in}, must be larger than η to maintain the interwall spacing constant. This means that the B-B bonds in the flattened (13,0)@(21,0) DWBNNT are stronger than those in the flattened (13,0) SWBNNT under the same η, resulting in a larger decrease in E_{CBM} in the former than in the latter.

It should be noted that the (5,0)@(13,0) DWBNNT and (5,0)@(13,0)@(21,0) TWBNNT show different changes in CBM charge densities from those of the SWBNNTs and (13,0)@(21,0) DWBNNT (Fig. 8). First, the CBM charge densities gradually transfer from boron atoms in the innermost tube to boron atoms in the second innermost tube. This charge delocalization and spreading account for the increase in E_{CBM} in the (5,0)@(13,0) DWBNNT and (5,0)@(13,0)@(21,0) TWBNNT during the early stage of the deformation. Then, overlap of the charge densities in curved regions in the second innermost tube is induced with increasing deformation. Consequently, E_{CBM} of the (5,0)@(13,0)

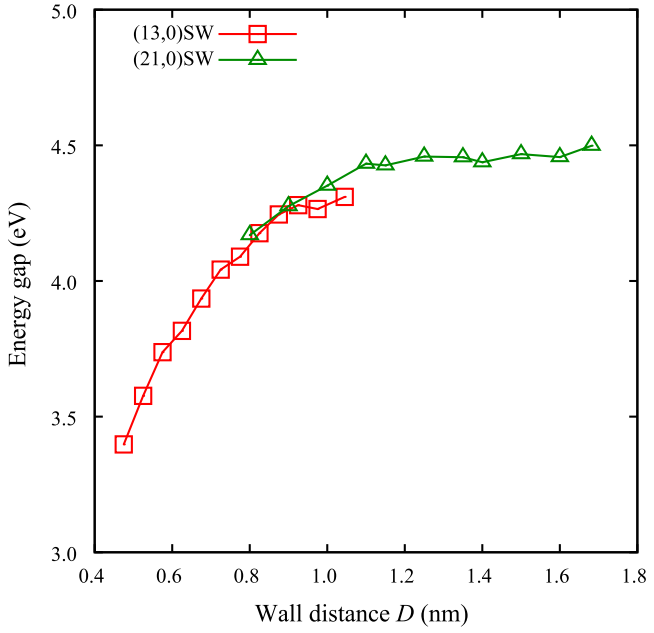

FIG. 6. (Color online) Energy gap of (13,0) and (21,0) SWBNNTs as a function of imaginary wall distance.

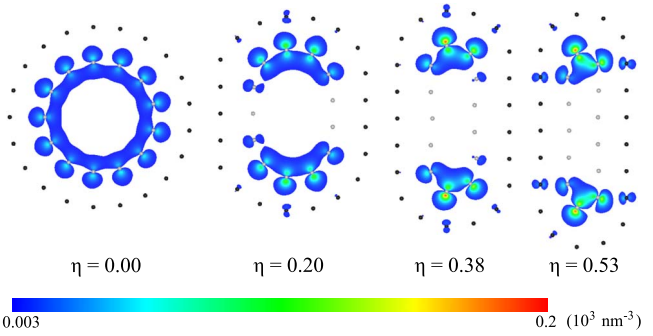

FIG. 7. (Color online) Change in the CBM charge density of (13,0)@(21,0) DWBNNT during flattening deformation.

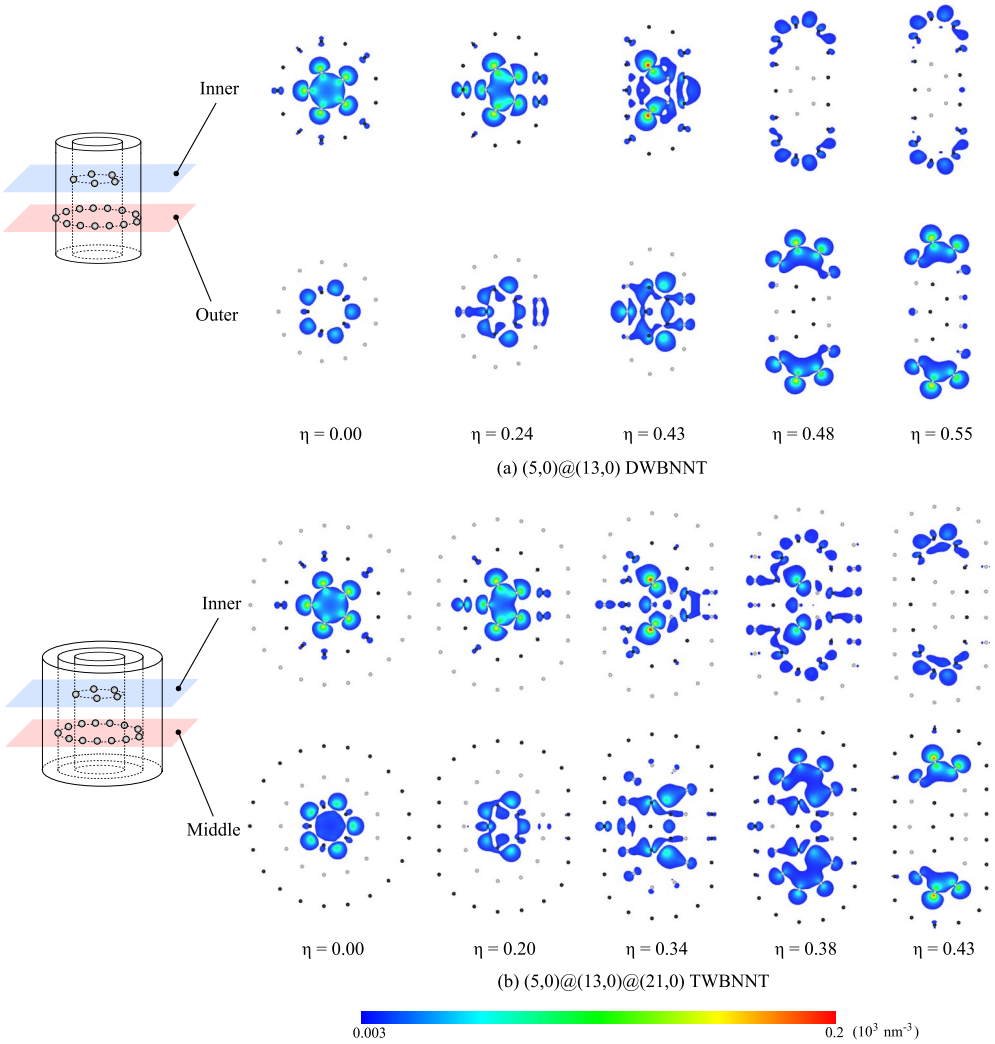

FIG. 8. (Color online) Change in the CBM charge density of (5,0)@(13,0) DWBNNT and (5,0)@(13,0)@(21,0) TWBNNT during flattening deformation.

DWBNNT and (5,0)@(13,0)@(21,0) TWBNNT decreases later in the deformation. It is this mechanism that results in the initial increase and subsequent decrease in E_g in the (5,0)@(13,0) DWBNNT and (5,0)@(13,0)@(21,0) TWBNNT. Because the latter has a larger η_{in} than the former under the same η (see the atomic positions in the innermost tube at η of 0.43 in Fig. 8), charge spreading from the first to the second innermost tube is completed earlier in the latter. Therefore, the latter shows an earlier shift from increase to decrease in E_g.

It is evident that a critical chiral index, $(n_c,0)$, exists for flattened zigzag MWBNNTs. Consider the innermost tube of a zigzag MWBNNT, denoted as $(n_{in},0)$. In the case of $n_{in} > n_c$, E_g decreases monotonically as the flattening deformation increases. In the reverse case $(n_{in} < n_c)$, E_g first increases and then decreases. From the results obtained in this research, n_c is proven to be an integer between 5 and 13. Furthermore, if zigzag BNNTs have the same n_{in}, a zigzag BNNT containing more walls shows a more rapid change in E_g [compared with the change in E_g between (13,0) SW and (13,0)@(21,0) DWBNNTs and between (5,0)@(13,0) DW and (5,0)@(13,0)@(21,0) TWBNNTs in Fig. 4].

In the aforementioned experimental study on a bent MWBNNT, a notable tendency for a zigzag atomic arrangement and local flattening have been observed.[16] Judging from the HRTEM images, n_{in} of the MWBNNT is larger than n_c. Therefore, it can be said that a possible reason for the change from insulating to semiconducting in the bent MWBNNT is electronic changes, as shown in Fig. 7. To the best of our knowledge, there has been no experimental study on deformed BNNTs with $n_{in} < n_c$ but we believe that the results for the (5,0)@(13,0) DWBNNT and (5,0)@(13,0)@(21,0) TWBNNT we obtained in this study are good predictions. Bending experiments on BNNTs with $n_{in} < n_c$ are greatly anticipated. Recently, Barboza *et al.*[30] have experimentally performed direct flattening compression of a SWCNT by means of an AFM tip and observed electronic changes in the SWCNT. We strongly expect that the same or a similar technique will also apply to BNNTs for comparing our results more directly and precisely with experimental ones.

IV. CONCLUSIONS

In the present research, electronic structures of flattened SW and MW BNNTs with the zigzag chiral index $(n,0)$ were investigated by first-principles DFT calculations. The key findings obtained are summarized as follows: (i) when the chiral index of the innermost tube, n_{in}, of a zigzag MWBNNT is larger than the critical one, n_c, the energy gap decreased monotonically with increasing flattening compression. (ii) When $n_{in}<n_c$, the energy gap first increased and then decreased with increasing flattening compression. This initial increase and subsequent decrease were caused by a charge spreading from the first to the second innermost tube and by bond formation in curved regions in the second innermost tube, respectively. (iii) The n_c was found to be an integer between 5 and 13.

Some remaining issues are how the other deformation modes affect electronic structures of BNNTs and how much force is required to deform a BNNT. Electronic changes in tensile- or torsion-deformed BNNTs and relationships between the energy gap and force will be presented elsewhere in the near future.

ACKNOWLEDGMENT

This work was supported in part by a Grant-in-Aid for Young Scientists (Start-up) No. 20810014 from Japan Society for the Promotion of Science.

*kinoshita@mech.nagoya-u.ac.jp

[1] N. G. Chopra, R. J. Luyken, K. Cherrey, V. H. Crespi, M. L. Cohen, S. G. Louie, and A. Zettl, Science **269**, 966 (1995).
[2] T. Oku, N. Koi, and K. Suganuma, J. Phys. Chem. Solids **69**, 1228 (2008).
[3] S. Iijima, Nature (London) **354**, 56 (1991).
[4] A. Rubio, J. L. Corkill, and M. L. Cohen, Phys. Rev. B **49**, 5081 (1994).
[5] X. Blase, A. Rubio, S. G. Louie, and M. L. Cohen, Europhys. Lett. **28**, 335 (1994).
[6] D. Golberg, Y. Bando, C. Tang, and C. Zhi, Adv. Mater.(Weinheim, Ger.) **19**, 2413 (2007).
[7] D. Golberg, Y. Bando, K. Kurashima, and T. Sato, Chem. Phys. Lett. **323**, 185 (2000).
[8] D. Golberg, Y. Bando, K. Kurashima, and T. Sato, Solid State Commun. **116**, 1 (2000).
[9] D. Golberg, Y. Bando, L. Bourgeois, K. Kurashima, and T. Sato, Appl. Phys. Lett. **77**, 1979 (2000).
[10] D. Golberg, Y. Bando, K. Kurashima, and T. Sato, Diamond Relat. Mater. **10**, 63 (2001).
[11] D. Golberg and Y. Bando, Appl. Phys. Lett. **79**, 415 (2001).
[12] S. Okada, S. Saito, and A. Oshiyama, Phys. Rev. B **65**, 165410 (2002).
[13] N. G. Chopra and A. Zettl, Solid State Commun. **105**, 297 (1998).
[14] T. Dumitrica, H. F. Bettinger, G. E. Scuseria, and B. I. Yakobson, Phys. Rev. B **68**, 085412 (2003).
[15] D. Golberg, Y. Bando, K. Kurashima, and T. Sato, Scr. Mater. **44**, 1561 (2001).
[16] X. Bai, D. Golberg, Y. Bando, C. Zhi, C. Tang, M. Mitome, and K. Kurashima, Nano Lett. **7**, 632 (2007).
[17] Y. H. Kim, K. J. Chang, and S. G. Louie, Phys. Rev. B **63**, 205408 (2001).
[18] Y. J. Peng, L. Y. Zhang, Q. H. Jin, B. H. Li, and D. T. Ding, Physica E (Amsterdam) **33**, 155 (2006).
[19] S. H. Jhi, D. J. Roundy, S. G. Louie, and M. L. Cohen, Solid State Commun. **134**, 397 (2005).
[20] G. Kresse and J. Hafner, Phys. Rev. B **47**, 558 (1993).
[21] G. Kresse and J. Furthmuller, Phys. Rev. B **54**, 11169 (1996).
[22] D. Vanderbilt, Phys. Rev. B **41**, 7892 (1990).
[23] J. P. Perdew and Y. Wang, Phys. Rev. B **45**, 13244 (1992).
[24] H. D. Monkhorst and J. D. Park, Phys. Rev. B **13**, 5188 (1976).
[25] A. P. M. Barboza, H. Chacham, and B. R. A. Neves, Phys. Rev. Lett. **102**, 025501 (2009).
[26] X. Blase, A. Rubio, S. G. Louie, and M. L. Cohen, Phys. Rev. B **51**, 6868 (1995).
[27] B. Arnaud, S. Lebègue, P. Rabiller, and M. Alouani, Phys. Rev. Lett. **96**, 026402 (2006).
[28] L. Wirtz, A. Marini, and A. Rubio, Phys. Rev. Lett. **96**, 126104 (2006).
[29] C. H. Park, C. D. Spataru, and S. G. Louie, Phys. Rev. Lett. **96**, 126105 (2006).
[30] A. P. M. Barboza, A. P. Gomes, B. S. Archanjo, P. T. Araujo, A. Jorio, A. S. Ferlauto, M. S. C. Mazzoni, H. Chacham, and B. R. A. Neves, Phys. Rev. Lett. **100**, 256804 (2008).